Asymmetric Bounded Neural Control for an Uncertain Robot by State Feedback and Output Feedback

Linghuan Kong, Wei He, *Senior Member, IEEE,* Yiting Dong, *Student Member, IEEE,* Long Cheng, *Senior Member, IEEE,* Chenguang Yang, *Senior Member, IEEE,* Zhijun Li, *Senior Member, IEEE*

***Abstract*—In this paper, an adaptive neural bounded control scheme is proposed for an n-link rigid robotic manipulator with unknown dynamics. With combination of neural approximation and backstepping technique, an adaptive neural network control policy is developed to guarantee the tracking performance of the robot. Different from the existing results, the bounds of the designed controller are known *a priori*, and they are determined by controller gains, *making them applicable within actuator limitations*. Furthermore, the designed controller is also able to compensate the effect of unknown robotic dynamics. Via Lyapunov stability theory, it can be proved that all the signals are uniformly ultimately bounded (UUB). Simulations are carried out to verify the effectiveness of the proposed scheme.**

***Index Terms*—Neural networks, Asymmetrically bounded inputs, A robotic manipulator, Adaptive control**

I. Introduction

Robots have a wide range of applications in various fields such as prospecting, navigation, aviation and so on [1]–[8]. Control design and stability analysis for a robot are increasingly important and have received considerable attention [9], [10]. A significant topic in the robot field is trajectory tracking [11]. Thus, many research results have been obtained in the past decades [12]–[14]. However, an avoidable challenge for controller design is that there exists model uncertainty due to the fact that robots are highly nonlinear and strongly coupled [15]–[18].

Model-based control has been proved to be effective in practical applications. An inevitable shortcoming for model-based control is that the dynamic information of the controlled system is required to be completely known. For a practical robot, accurate dynamic information is hardly possible to obtain such that model-based controller cannot be directly applied to real implementation. Due to requiring little knowledge [19]–[33], learning control has been widely utilized in control theory and applications to handle system uncertainty. Neural networks serve as a powerful tool to model system uncertainty in a real-time way, which have been widely used for solving the control problems of unknown nonlinear systems [34]–[49]. and are used for complex defects on magnetic flux leakage [50]. In [51], an adaptive neural network control scheme is developed for strict-feedback nonlinear state constrained systems in the presence of input delay and system uncertainty. In [52], neural networks are employed to approximate system uncertainty of multi-input-multi-output nonlinear systems. In [53], an adaptive neural network control method is proposed for unknown nonlinear systems with full-state constraints. In [54], adaptive neural networks are used to deal with the tracking problem for rigid robotic manipulators with uncertainty and output constraints. In most situations, velocity signals are exceedingly difficult or even impossible to measure. Then researchers try to design the state observer to estimate the immeasurable states, and many research results have been carried out [55], [56]. In [57], a state observer is designed to estimate the immeasurable states such that an adaptive neural output feedback control is developed for large-scale stochastic nonlinear systems. In [58], the high-gain observer estimates the velocity signals for an n-link rigid robotic manipulator, and an adaptive output feedback control scheme is developed.

Input saturation exists in most practical robots, which, if not properly coped with, would degrade system performances and even cause instability [59]–[65]. Recently, input saturation has been received considerable attention from analysis and controller design, and furthermore many research results have been derived [66]–[70]. In [66], an auxiliary variable is designed for nonlinear systems with nonsymmetric input saturations and time delays to eliminate the effect of input saturation. In [67], the control problems of multiple strict-feedback nonlinear systems with saturation nonlinearity are discussed, where hyperbolic tangent function $tanh(\cdot)$ is introduced to approximate saturation nonlinearity. In [68], adaptive neural network control is proposed for a class of nonlinear systems with asymmetric saturation actuators. In [69], an adaptive fuzzy control approach is presented for uncertain nonstrict-

This work was supported in part by the National Natural Science Foundation of China under Grant 61873298, Grant 61873268, Grant 61633016, Grant 61751310 and Grant 61573147, in part by the Anhui Science and Technology Major Program under Grant 17030901029, in part by the Beijing Science and Technology Project (Grant No. Z181100003118006), in part by the Beijing Municipal Natural Science Foundation (Grant No. L182060), and in part by the Engineering and Physical Sciences Research Council (EPSRC) under Grant EP/S001913.

L. Kong and W. He are with School of Automation and Electrical Engineering, University of Science and Technology Beijing, Beijing 100083, China, and also with the Institute of Artificial Intelligence, University of Science and Technology Beijing, Beijing 100083, China. (Email: weihe@ieee.org)

Y. Dong is with the Department of Mechanical Engineering, Texas Tech University, Lubbock, TX 79409, USA.

L. Cheng is with the State Key Laboratory of Management and Control for Complex Systems, Institute of Automation, Chinese Academy of Sciences, Beijing 100190, China, and also with the University of the Chinese Academy of Sciences, Beijing 100049, China.

C. Yang is with Bristol Robotics Laboratory, University of the West of England, Bristol, BS16 1QY, UK.

Z. Li is with Department of Automation, University of Science and Technology of China, Hefei, China.

feedback systems with input saturation. In [70], a novel adaptive sliding mode controller is designed for Takagi-Sugeno fuzzy systems with actuator saturation and system uncertainty. An asymmetric saturation situation may be encountered if the actuators partially loss their effectiveness for an uncertain robot, due to motor fault, change of mechanical structure, etc, which drives us to solve the asymmetric saturation constraint problems for an uncertain robot. In [66]–[70], the bounds of the designed controller are considered to be unknown for the controller design, which motivates us to further investigate the adaptive neural network control with asymmetric and known bounds for an n-link rigid robotic manipulator with uncertain dynamics, making the designed controller applicable within actuator limitations.

Motivated by above observations, this paper focuses on the adaptive bounded control for an n-link rigid robotic manipulator with unknown dynamics, where the bounds of the designed controller are asymmetric and known *a prior* and furthermore can be predetermined by changing control gains, *making the designed controller applicable within actuator limitations*. Neural networks are employed to approximate unknown robotic dynamics. A high-gain observer is introduced to estimate the immeasurable states.

Compared with the previous works, the main contributions are summarized as follows:

1) Compared with [66]–[70], a main feature in this paper is that the bounds of the designed controller are asymmetric and known *a priori*, and furthermore they are predetermined by changing control gains.
2) In [66], an additional auxiliary variable is designed to eliminate the effect of input saturation. Compared with [66], we directly adopt hyperbolic tangent function *tanh*$(\cdot)$ to obtain the bounded control. Thus, the structure of the designed controller in this paper may be more simpler to some extent, which is beneficial to controller implementation and real-time control.

The structure of the paper is presented. Section II shows preliminaries and problem formulation. The main results are given in Section III. In Section IV, some simulation examples are provided to demonstrate the effectiveness of the proposed method. Finally, Section V concludes this paper.

Notations 1: Let $\| \bullet \|$ be the Euclidean norm of a vector or a matrix. Let $\mathcal{A}_i$ $(i = 1, \ldots, n)$ denote the ith row and the ith diag element $\mathcal{A}_{ii}$ of the vector $\mathcal{A} \in \mathbb{R}^n$ and the matrix $\mathcal{A} \in \mathbb{R}^{n \times n}$, respectively. The symbol "I" is used to denote an identity matrix with appropriate dimensions.

II. Preliminaries and Problem Formulation

A. Problem Formulation

Consider an n-link rigid robotic manipulator model [71] in joint space as

$$M(q)\ddot{q} + C(q,\dot{q})\dot{q} + G(q) = \mu \tag{1}$$

where $q \in \mathbb{R}^n$, $\dot{q} \in \mathbb{R}^n$, $\ddot{q} \in \mathbb{R}^n$ denote the vector of joint position, velocity and acceleration, $M(q) \in \mathbb{R}^{n\times n}$ denotes the positive definite quality inertia matrix, $C(q,\dot{q}) \in \mathbb{R}^{n\times n}$ denotes the coriolis and centrifugal matrix, $G(q) \in \mathbb{R}^n$ denotes the gravitational forces, $\mu \in \mathbb{R}^n$ denotes the control torque vector and satisfies

$$\mu_{ci}^- \le \mu_i \le \mu_{ci}^+ \tag{2}$$

where $\mu_{ci}^+ \in \mathbb{R}^+$, $\mu_{ci}^- \in \mathbb{R}^-$, $i = 1, \ldots, n$, denote the upper and lower bound of μ_i, respectively.

The control objective in this paper is to design an asymmetrically bounded control scheme ensuring: 1) the robot given in (1) can track the reference trajectory x_d with an acceptable accuracy; 2) tracking errors are uniformly ultimately bounded (UUB).

Assumption 1: [72] System matrixes $M(q)$, $C(q,\dot{q})$ and $G(q)$ are unknown, and furthermore $M^{-1}(q)$ exists.

Property 1: [72] $\dot{M}(q) - 2C(q,\dot{q})$ is a skew symmetric matrix. $\forall x \in \mathbb{R}^n$, $x^T(\dot{M}(q) - 2C(q,\dot{q}))x = 0$.

B. Radial Basis Function Neural Networks (RBFNNs)

In the consequent design, unknown nonlinear functions would be approximated by RBFNNs in the following form.

$$h_n(Z) = \hat{\theta}^T \varphi(Z) \tag{3}$$

where $h_n(Z)$ is any nonlinear function, $Z \in \Omega_Z \subset \mathbb{R}^q$ is the input vector, $\hat{\theta} = [\hat{\theta}_1, \ldots, \hat{\theta}_l]^T \in \mathbb{R}^l$ is the weight vector, $l > 1$ is the neural network node number, and $\varphi(Z) = [\varphi_1(Z), \ldots, \varphi_l(Z)]^T$ with $\varphi_i(Z)$ chosen as the Gaussian radial basis function. $\varphi_i(Z)$ is given by

$$\varphi_i(Z) = \exp[\frac{-(Z-\varrho_i)^T(Z-\varrho_i)}{\eta_i^2}] \tag{4}$$

where $\varrho_i = [\varrho_{i1}, \ldots, \varrho_{iq}]^T$ is the center of the receptive field and η_i is the width of the Gaussian radial basis function, $i = 1, \ldots, n$.

Lemma 1: [73] For given accuracy $\epsilon > 0$ with sufficiently large node number l, neural networks (3) can approximate any continuous nonlinear function $h(Z)$ defined in the compact set $\Omega \subset \mathbb{R}^q$ such that

$$h(Z) = \theta^T \varphi(Z) + \epsilon(Z), \quad \forall Z \in \Omega \subset \mathbb{R}^q \tag{5}$$

where θ is the optimal weight defined as

$$\theta := \arg \min_{\hat{\theta} \subset \mathbb{R}^l} \left\{ \sup_{Z \in \Omega} |h(Z) - \hat{\theta}^T \varphi(Z)| \right\}, \tag{6}$$

and $\epsilon(Z)$ is the approximation error satisfying $\|\epsilon(Z)\| \le \bar{\epsilon}$ with $\bar{\epsilon}$ being positive constants.

Lemma 2: [73] Given that the Gaussian radial basis function with $\hat{Z} = Z - \bar{\gamma}\nu$ being the input vector, where ν is a bounded vector and $\bar{\gamma}$ is a positive constant, then we have

$$\varphi_i(\hat{Z}) = \exp[\frac{-(\hat{Z}-\varrho_i)^T(\hat{Z}-\varrho_i)}{\eta_i^2}], \quad i = 1, \ldots, l \tag{7}$$

$$\varphi(\hat{Z}) = \varphi(Z) + \bar{\gamma}\varphi \tag{8}$$

$$\|\varphi(Z)\|^2 \le l \tag{9}$$

where φ is a bounded function vector.

C. Useful Properties, Definitions and Lemmas

Property 2: [72] $\mathcal{A} \in \mathbb{R}^{n\times n}$ is a symmetric positive definite matrix. $\lambda_{\min}(\mathcal{A})$ and $\lambda_{\max}(\mathcal{A})$ are the minimum and maximum eigenvalues of $\mathcal{A}$. For $\forall x \in \mathbb{R}^n$, there is $\lambda_{\min}(\mathcal{A})||x||^2 \leq x^T\mathcal{A}x \leq \lambda_{\max}(\mathcal{A})||x||^2$.

η_i, $i = 1, \ldots, n$,

Definition 1: Define the diagonal matrix $\mathrm{Tanh}^2(.) \in \mathbb{R}^{n\times n}$ as follows:

$$\mathrm{Tanh}^2(\eta) = \mathrm{diag}[\tanh^2(\eta_1), \ldots, \tanh^2(\eta_n)] \tag{10}$$

where $\eta = [\eta_1, \ldots, \eta_n]^T \in \mathbb{R}^n$.

Lemma 3: Assume that $f(\mu)$ is an asymmetric saturation function represented as

$$f(\mu) = \begin{cases} \mu_c^+ & \text{if } \mu_c^+ < \mu \\ \mu & \text{if } \mu_c^- \leq \mu \leq \mu_c^+ \\ \mu_c^- & \text{Otherwise} \end{cases} \tag{11}$$

where μ_c^+ and μ_c^- are the upper and lower bound of μ, respectively. When $\mu = \mu_c^+$ or $\mu = \mu_c^-$, there is a sharp corner. Then a novel smooth function is introduced to approximate this saturation function in the following form.

$$f(\mu) = \delta\mu_c^+ \tanh(\frac{\mu}{\mu_c^+}) + (1-\delta)\mu_c^- \tanh(\frac{\mu}{\mu_c^-}) + p(\mu) \tag{12}$$

where δ denotes a switching function defined as [74]

$$\delta = \begin{cases} 1 & \text{if } \mu \geq 0 \\ 0 & \text{Otherwise} \end{cases} \tag{13}$$

and $p(\mu)$ denotes a bounded function. Then we present a proof showing that $p(\mu)$ is bounded.

Proof: Two cases are considered as follows:

- Case one: $\mu > \mu_c^+$. (12) is rewritten as $f(\mu) = \mu_c^+ \tanh(\frac{\mu}{\mu_c^+}) + p(\mu)$. With combination of (11), it follows that $|p(\mu)| = |\mu_c^+(1 - \tanh(\frac{\mu}{\mu_c^+}))| \leq |\mu_c^+|$, which illustrates that $p(\mu)$ is bounded for the case $\mu > \mu_c^+$. Similar proof can also be presented for the case $\mu_c^- > \mu$.
- Case two: $0 \leq \mu \leq \mu_c^+$. (12) is rewritten as $f(\mu) = \mu_c^+ \tanh(\frac{\mu}{\mu_c^+}) + p(\mu)$. With combination of (11), it follows that $p(\mu) = \mu - \mu_c^+ \tanh(\frac{\mu}{\mu_c^+}) \leq \mu_c^+(1 - \tanh(\frac{\mu}{\mu_c^+}))$, similarly, implying that $p(\mu)$ is bounded when $0 \leq \mu \leq \mu_c^+$. Similar proof can also be presented for the case $\mu_c^- \leq \mu < 0$.

III. Control Design

For the convenience of controller design, before controller design, we define $x_1 = q$ and $x_2 = \dot{q}$, and then (1) can be rewritten as

$$\dot{x}_1 = x_2 \tag{14}$$

$$\dot{x}_2 = M^{-1}(\mu - G - Cx_2) \tag{15}$$

where $x_1 = [x_{11}, \ldots, x_{1n}]^T$, $x_2 = [x_{21}, \ldots, x_{2n}]^T$. In the subsequent design, M, C and G denote $M(x_1)$, $C(x_1, x_2)$ and $G(x_1)$, respectively.

A. Model-based Control Design

Tracking errors are defined as

$$z_1 = x_1 - x_d \tag{16}$$

$$z_2 = x_2 - \alpha \tag{17}$$

where α is defined as

$$\alpha = -A + \dot{x}_d \tag{18}$$

where $A = [\frac{k_1 \ln\cosh(z_{11})}{\tanh(z_{11}}, \ldots, \frac{k_n \ln\cosh(z_{1n})}{\tanh(z_{1n})}]^T \in \mathbb{R}^n$, and $K = \mathrm{diag}[k_1, \ldots, k_n] \in \mathbb{R}^{n\times n}$ is a positive definite matrix. Then error dynamics is calculated as

$$\dot{z}_1 = z_2 - A \tag{19}$$

$$\dot{z}_2 = M^{-1}(\mu - G - Cx_2) - \dot{\alpha} \tag{20}$$

Choose a positive Lyapunov function candidate as

$$V_1 = \sum_{i=1}^{n} \ln(\cosh(z_{1i})) + \frac{1}{2}z_2^T M z_2 \tag{21}$$

Substituting (19) and (20) into the time derivative of (21), we get

$$\begin{aligned}\dot{V}_1 = &-\sum_{i=1}^{n} k_i \ln(\cosh(z_{1i})) + \sum_{i=1}^{n} z_{2i}\tanh(z_{1i}) \\ &+ z_2^T(\mu - G - C\alpha - M\dot{\alpha})\end{aligned} \tag{22}$$

Then, model-based control μ is designed as

$$\mu = -\tanh(z_1) - K_1\tanh(z_2) + B\tanh(B^{-1}\psi) \tag{23}$$

where $\mu = [\mu_1, \ldots, \mu_n]^T \in \mathbb{R}^n$, $K_1 = \mathrm{diag}[k_{11}, \ldots, k_{1n}] \in \mathbb{R}^{n\times n}$ is a positive definite matrix, and $B = \mathrm{diag}[\delta_i\mu_i^+ + (1-\delta_i)\mu_i^-] \in \mathbb{R}^{n\times n}$ with μ_i^- being negative constants and μ_i^+ being positive constants. It should be emphasized that μ_i^- and μ_i^+ are also considered as adjustable control gains. Auxiliary variable ψ is defined as

$$\begin{aligned}\psi_i = &\delta_i\mu_i^+ \mathrm{arctanh}\left(\frac{(G + C\alpha + M\dot{\alpha})_i}{\mu_i^+}\right) \\ &+ (1-\delta_i)\mu_i^- \mathrm{arctanh}\left(\frac{(G + C\alpha + M\dot{\alpha})_i}{\mu_i^-}\right)\end{aligned} \tag{24}$$

where $\mathrm{arctanh}(\cdot)$ denotes the inverse function of $\tanh(\cdot)$, and $\psi = [\psi_1, \ldots, \psi_n]^T \in \mathbb{R}^n$. We assume that initial values satisfy $\mu_i^- < (G + C\alpha + M\dot{\alpha})_i(0) < \mu_i^+$. δ_i is a switching function defined as

$$\delta_i = \begin{cases} 1 & \text{if } (G + C\alpha + M\dot{\alpha})_i > 0 \\ 0 & \text{Otherwise} \end{cases} \tag{25}$$

Substituting (23) into (22), we get

$$\begin{aligned}\dot{V}_1 = &-\sum_{i=1}^{n} k_i \ln(\cosh(z_{1i})) - z_2^T K_1 \tanh(z_2) \\ &+ z_2^T(B\tanh(B^{-1}\psi) - G - C\alpha - M\dot{\alpha})\end{aligned} \tag{26}$$

Define $f(\mu) = G + C\alpha + M\dot{\alpha}$, and by ultilizing Lemma 3, we have $f(\mu) = B\tanh(B^{-1}\psi) + p(\mu)$, where $p(\mu)$ denotes the approximation error, and furthermore it is assumed that $p(\mu)$ is upper bounded, i.e., $\|p(\mu)\| \leq \bar{p}$ with $\bar{p}$ being unknown positive constants. Thus we have $z_2^T(B\tanh(B^{-1}\psi) - G - C\alpha - M\dot{\alpha}) = -z_2^T p(\mu) \leq \frac{1}{2}z_2^T z_2 + \frac{1}{2}\bar{p}^2$. According to Taylor expansion, we know

$$\tanh(z_2) = z_2 + o(z_2), \quad \|z_2\| < \frac{\pi}{2} \tag{27}$$

where $o(z_2) = -\frac{1}{3}z_2^3 + \frac{2}{15}z_2^5 - \frac{17}{315}z_2^7 + \cdots$, and in the interval $\|z_2\| < \frac{\pi}{2}$, $o(z_2)$ is bounded, i.e., $\|o(z_2)\| \leq \bar{o}$ with $\bar{o}$ being a positive constant. With aid of Young's inequality, thus (26) becomes

$$\begin{aligned}\dot{V}_1 =& -\sum_{i=1}^{n} k_i \ln(\cosh(z_{1i})) - z_2^T K_1 z_2 - z_2^T K_1 o(z_2) \\ &+ \frac{1}{2}z_2^T z_2 + \frac{1}{2}\bar{p}^2 \\ \leq& -\kappa_1 V_1 + C_1\end{aligned} \tag{28}$$

where $\kappa_1 = \min\left\{\min_{i=1,\ldots,n} k_i, \frac{\lambda_{\min}(K_1 - I)}{\lambda_{\max}(M)}\right\}$, $C_1 = \frac{1}{2}\lambda_{\max}(K_1^T K_1)\bar{o}^2 + \frac{1}{2}\bar{p}^2$. To ensure $\kappa_1 > 0$, controller parameters should satisfy $\min_{i=1,\ldots,n} k_i > 0$ and $\lambda_{\min}(K_1 - I) > 0$. Then the following theorem is obtained.

Theorem 1: For robotic system (1), by designing model-based control input (23), the controller can ensure that all the error signals are UUB. Furthermore, z_1 eventually converges to the compact set defined as $\Omega_{z_1} := \left\{z_1 \in \mathbb{R}^n \middle| |z_{1i}| \leq \sqrt{2e^{H_1}}, i = 1, \ldots, n\right\}$, and z_2 eventually converges to the compact set defined as $\Omega_{z_2} := \left\{z_2 \in \mathbb{R}^n \middle| \|z_2\| \leq \sqrt{\frac{2H_1}{\lambda_{\min}(M)}}\right\}$, where $H_1 = V_1(0) + \frac{C_1}{\kappa_1}$.

Proof: See Appendix

Remark 1: If $\delta_i = 1$, (23) can be rewritten as $\mu_i = -\tanh(z_{1i}) - k_{1i}\tanh(z_{2i}) + \mu_i^+ \tanh(\frac{\psi_i}{\mu_i^+})$, $i = 1, \ldots, n$, and by the utilization of the property of the continuous function $\tanh(\cdot)$, we know that μ_i is upper bounded, i.e., $\mu_i \leq 1 + k_{1i} + \mu_i^+$. If $\delta_i = 0$, (23) can reduce to $\mu_i = -\tanh(z_{1i}) - k_{1i}\tanh(z_{2i}) + \mu_i^- \tanh(\frac{\psi_i}{\mu_i^-})$, $i = 1, \ldots, n$, and we further know that μ_i is also lower bounded, i.e., $\mu_i \geq -(1 + k_{1i} + \mu_i^-)$. Then, defining $\mu_{ci}^+ = 1 + k_{1i} + \mu_i^+$ and $\mu_{ci}^- = -(1 + k_{1i} + \mu_i^-)$ implies $\mu_{ci}^- \leq \mu_i \leq \mu_{ci}^+, i = 1, \ldots, n$. It should be noted that k_{1i}, μ_i^+ and μ_i^-, $i = 1, \ldots, n$ can also be considered as controller gains, which, if necessary, may also change for both satisfactory tracking performances and suitable bounds of controllers, making the controller applicable within actuator limitations.

B. State-Feedback-Based Adaptive Neural Control Design

Assume that M, C and G are unknown such that model-based control (23) is unavailable in practice. Furthermore, auxiliary variable ψ given in (24) is also unknown. Then neural networks are employed to approximate ψ in the following form.

$$\theta^T \varphi(Z) = \psi + \epsilon(Z) \tag{29}$$

where θ is the desired weight vector, $Z = [x_1^T, x_2^T, z_1^T, z_2^T]^T \in \mathbb{R}^{4n}$ is the input of RBFNNs, and $\epsilon(Z)$ is the approximation error satisfying $\|\epsilon(Z)\| \leq \bar{\epsilon}$ with $\bar{\epsilon}$ being a positive constant. Then an adaptive neural network controller is designed as

$$\mu = -\tanh(z_1) - K_1\tanh(z_2) + B\tanh(B^{-1}\hat{\psi}) \tag{30}$$

$$\hat{\psi} = \hat{\theta}^T \varphi(Z) \tag{31}$$

$$\dot{\hat{\theta}}_i = -\Gamma_i(\varphi(Z)z_{2i} + \varsigma\hat{\theta}_i), \quad i = 1, \ldots, n \tag{32}$$

where $K_1 = \mathrm{diag}[k_{11}, \ldots, k_{1n}] \in \mathbb{R}^{n\times n}$ is a positive definite matrix, $B = \mathrm{diag}[\delta_i\mu_i^+ + (1-\delta_i)\mu_i^-] \in \mathbb{R}^{n\times n}$ with δ_i defined as

$$\delta_i = \begin{cases} 1 & \text{if } \hat{\theta}_i^T\varphi(Z) \geq \ell_i \\ 0 & \text{Otherwise,} \end{cases} \tag{33}$$

$\ell_i \triangleq \tilde{\theta}_i^T\varphi(Z) + \epsilon_i(Z)$, $(\hat{\bullet})$ denotes the estimation of $(\bullet)$ satisfying $(\tilde{\bullet}) = (\hat{\bullet}) - (\bullet)$, Γ_i is a symmetric positive definite matrix, and ς is a small constant which improves the robustness.

Remark 2: Note that switching function δ_i given in (25) is based on an assumption that M, C and G are all known. However, in this section M, C and G are assumed to be unknown, which causes switching function δ_i given in (25) to be ineffective. Therefore switching function δ_i need redesigned again. Due to the fact that $\theta^T\varphi(Z) = \hat{\theta}^T\varphi(Z) - \tilde{\theta}^T\varphi(Z)$, (29) is rewritten as $\psi = \hat{\theta}^T\varphi(Z) - \tilde{\theta}^T\varphi(Z) - \epsilon(Z)$. Let us recall switching function δ_i given in (25) and consider the fact that $\mathrm{arctanh}(.)$ is an odd function, and we know: 1) when $(G + C\alpha + M\dot{\alpha})_i \geq 0$, it follows that $\psi_i \geq 0$ and $\hat{\theta}_i^T\varphi(Z) \geq \tilde{\theta}_i^T\varphi(Z) + \epsilon_i(Z)$; 2) when $(G + C\alpha + M\dot{\alpha})_i < 0$, it follows that $\psi_i < 0$ and $\hat{\theta}_i^T\varphi(Z) < \tilde{\theta}_i^T\varphi(Z) + \epsilon_i(Z)$. By defining $\ell_i = \tilde{\theta}_i^T\varphi(Z) + \epsilon_i(Z)$, one can obtain the switch function δ_i given in (33), $i = 1, \ldots, n$.

Similar to analysis in Remark 1, we can conclude that $\mu_i, i = 1, \ldots, n$ given in (30) are bounded, i.e., $\mu_{ci}^- \leq \mu_i \leq \mu_{ci}^+, i = 1, \ldots, n$, are guaranteed. A Lyapunov function candidate is chosen as

$$V_2 = \sum_{i=1}^{n}\ln(\cosh(z_{1i})) + \frac{1}{2}z_2^T M z_2 + \frac{1}{2}\sum_{i=1}^{n}\tilde{\theta}_i^T\Gamma_i^{-1}\tilde{\theta}_i \tag{34}$$

Substituting (19) and (20) into the time derivative of (34), we get

$$\begin{aligned}\dot{V}_2 =& -\sum_{i=1}^{n} k_i\ln(\cosh(z_{1i})) + \sum_{i=1}^{n} z_{2i}\tanh(z_{1i}) \\ &+ z_2^T(\mu - G - C\alpha - M\dot{\alpha}) + \sum_{i=1}^{n}\tilde{\theta}_i^T\Gamma_i^{-1}\dot{\hat{\theta}}_i\end{aligned} \tag{35}$$

Substituting (30) and (32) into (35), we further get

$$\begin{aligned}\dot{V}_2 =& -\sum_{i=1}^{n} k_i\ln(\cosh(z_{1i})) - \sum_{i=1}^{n}\tilde{\theta}_i^T(\varphi(Z)z_{2i} + \varsigma\hat{\theta}_i) \\ &- z_2^T K_1\tanh(z_2) + z_2^T(B\tanh(B^{-1}\hat{\psi}) \\ &- G - C\alpha - M\dot{\alpha})\end{aligned} \tag{36}$$

Define $f(\mu) = G + C\alpha + M\dot{\alpha}$, and by utilizing Lemma 3, we have $f(\mu) = B\tanh(B^{-1}\psi) + p(\mu)$, where $p(\mu)$ denotes the approximation error, and furthermore it is assumed that $p(\mu)$ is upper bounded, i.e., $\|p(\mu)\| \leq \bar{p}$ with $\bar{p}$ being unknown positive constants. Then we know that $z_2^T(B\tanh(B^{-1}\hat{\psi}) -$

$G-C\alpha-M\dot{\alpha})$ becomes $z_2^T B(\tanh(B^{-1}\hat{\psi})-\tanh(B^{-1}\psi))-z_2^T p(\mu)$. According to mean value theorem, we have

$$\tanh(B_i^{-1}\hat{\psi}_i)-\tanh(B_i^{-1}\psi_i) = (1-\tanh^2(\eta_i))(B_i^{-1}(\hat{\psi}_i-\psi_i)) \tag{37}$$

where $\eta_i \in (B_i^{-1}\hat{\psi}_i, B_i^{-1}\psi_i)$ or $\eta_i \in (B_i^{-1}\psi_i, B_i^{-1}\hat{\psi}_i)$ and $B^{-1}=\mathrm{diag}[B_1^{-1},\ldots,B_n^{-1}]$, $i=1,\ldots,n$. Using (29) and (31), we have $\tanh(B_i^{-1}\hat{\psi}_i)-\tanh(B_i^{-1}\psi_i)=(1-\tanh^2(\eta_i))B_i^{-1}(\tilde{\theta}_i^T\varphi(Z)+\epsilon_i(Z))$, $i=1,\ldots,n$. Therefore, (36) becomes

$$\begin{aligned}\dot{V}_2 =& -\sum_{i=1}^n k_i\ln(\cosh(z_{1i}))-\sum_{i=1}^n\tilde{\theta}_i^T(\varphi(Z)z_{2i}+\varsigma\hat{\theta}_i)\\ &-z_2^T K_1\tanh(z_2)+z_2^T(I-\mathrm{Tanh}^2(\eta))\\ &\times(\tilde{\theta}^T\varphi(Z)+\epsilon(Z))-z_2^T p(\mu)\end{aligned} \tag{38}$$

Note that $\sum_{i=1}^n\tilde{\theta}_i^T\varphi(Z)z_{2i}=z_2^T\tilde{\theta}^T\varphi(Z)$ and consider (27), we further have

$$\begin{aligned}\dot{V}_2 =& -\sum_{i=1}^n k_i\ln(\cosh(z_{1i}))-\sum_{i=1}^n\tilde{\theta}_i^T\varsigma\hat{\theta}_i-z_2^T K_1 z_2\\ &-z_2^T K_1 o(z_2)-z_2^T\mathrm{Tanh}^2(\eta)(\tilde{\theta}^T\varphi(Z)+\epsilon(Z))\\ &+z_2^T\epsilon(Z)-z_2^T p(\mu)\end{aligned} \tag{39}$$

In terms of Young's inequality, we obtain $z_2^T K_1 o(z_2) \le \frac{1}{2}z_2^T z_2+\frac{1}{2}\lambda_{\max}(K_1^T K_1)\bar{o}^2$, $-\sum_{i=1}^n\tilde{\theta}_i^T\varsigma\hat{\theta}_i \le -\frac{\varsigma}{2}\sum_{i=1}^n\tilde{\theta}_i^T\tilde{\theta}_i+\frac{\varsigma}{2}\sum_{i=1}^n\theta_i^T\theta_i$, $-z_2^T\mathrm{Tanh}^2(\eta)\tilde{\theta}^T\varphi(Z) \le \frac{\varrho_1^2}{2}z_2^T z_2+\frac{l^2}{2\varrho_1^2}\sum_{i=1}^n\tilde{\theta}_i^T\tilde{\theta}_i$, $-z_2^T\mathrm{Tanh}^2(\eta)\epsilon(Z)\le\frac{1}{2}z_2^T z_2+\frac{1}{2}\bar{\epsilon}^2$, $z_2^T\epsilon(Z)\le\frac{1}{2}z_2^T z_2+\frac{1}{2}\bar{\epsilon}^2$, and $-z_2^T p(\mu)\le\frac{1}{2}z_2^T z_2+\frac{1}{2}\bar{p}^2$, where ϱ_1 is an adjustable parameter. Thus, we have

$$\begin{aligned}\dot{V}_2 \le& -\sum_{i=1}^n k_i\ln(\cosh(z_{1i}))-z_2^T\left(K_1-(\frac{4+\varrho_1^2}{2})I\right)z_2\\ &-\frac{1}{2}\left(\varsigma-\frac{l^2}{\varrho_1^2}\right)\sum_{i=1}^n\tilde{\theta}_i^T\tilde{\theta}_i+\frac{1}{2}\lambda_{\max}(K_1^T K_1)\bar{o}^2\\ &+\frac{\varsigma}{2}\sum_{i=1}^n\theta_i^T\theta_i+\bar{\epsilon}^2+\frac{1}{2}\bar{p}^2\\ \le& -\kappa_2 V_2+C_2\end{aligned} \tag{40}$$

where

$$\begin{aligned}\kappa_2 =& \min\Bigg\{\min_{i=1,\ldots,n}k_i,\ \min_{i=1,\ldots,n}\left(\varsigma-\frac{l^2}{\varrho_1^2}\right)\frac{1}{\lambda_{\max}(\Gamma_i^{-1})},\\ &\lambda_{\min}\left(2K_1-(4+\varrho_1^2)I\right)\frac{1}{\lambda_{\max}(M)}\Bigg\}\\ C_2 =& \frac{1}{2}\lambda_{\max}(K_1^T K_1)\bar{o}^2+\frac{\varsigma}{2}\sum_{i=1}^n\theta_i^T\theta_i+\bar{\epsilon}^2+\frac{1}{2}\bar{p}^2\end{aligned}$$

To guarantee $\kappa_2>0$, controller parameters should be chosen to satisfy: $\min_{i=1,\ldots,n}k_i>0$, $\min_{i=1,\ldots,n}\left(\varsigma-\frac{l^2}{\varrho_1^2}\right)>0$ and $\lambda_{\min}\left(2K_1-(4+\varrho_1^2)I\right)>0$. Then the following theorem is obtained.

Theorem 2: For robotic system (1), by designing adaptive neural network controller (30) with adaptive law (32), the controller can ensure that all the error signals are UUB. Furthermore, z_1 eventually converges to the compact set defined as $\Omega_{z_1} := \left\{z_1\in\mathbb{R}^n \middle| |z_{1i}|\le\sqrt{2e^{H_2}}, i=1,\ldots,n\right\}$, and z_2 eventually converges to the compact set defined as $\Omega_{z_2} := \left\{z_2\in\mathbb{R}^n \middle| ||z_2||\le\sqrt{\frac{2H_2}{\lambda_{\min(M)}}}\right\}$, where $H_2=V_2(0)+\frac{C_2}{\kappa_2}$.

Proof: The proof is similar to that of Theorem 1, so it will not be discussed in details.

C. Output-Feedback-Based Adaptive Neural Control Design

Assume that velocity signal x_2 is immeasurable. We will introduce a high-gain observer to estimate x_2. x_2 is estimated by $\hat{x}_2=\frac{\pi_2}{\rho}$. Estimate error is defined as $\tilde{z}_2=\frac{\pi_2}{\rho}-x_2$ and is said to be bounded [73], i.e., $\|\tilde{z}_2\|\le\bar{z}$ with $\bar{z}$ being a positive constant. Dynamics of π_2 is given as

$$\rho\dot{\pi}_1=\pi_2, \tag{41}$$

$$\rho\dot{\pi}_2=-\lambda_1\pi_2-\pi_2+x_1 \tag{42}$$

where λ_1 is a constant satisfying that $\lambda_1 s+1$is Hurwitz, and ρ is a number. An adaptive neural controller is designed as

$$\mu=-\tanh(z_1)-K_1\tanh(\hat{z}_2)+B\tanh(B^{-1}\hat{\psi}) \tag{43}$$

$$\hat{\psi}=\hat{\theta}^T\varphi(\hat{Z}) \tag{44}$$

$$\dot{\hat{\theta}}_i=-\Gamma_i(\varphi(\hat{Z})\hat{z}_{2i}+\varsigma\hat{\theta}_i),\quad i=1,\ldots,n \tag{45}$$

where $K_1=\mathrm{diag}[k_{11},\ldots,k_{1n}]\in\mathbb{R}^{n\times n}$ is a positive definite matrix, $\hat{Z}=[x_1^T,\hat{x}_2^T,z_1^T,\hat{z}_2^T]^T\in\mathbb{R}^{4n}$, $\hat{z}_2=\frac{\pi_2}{\rho}-\alpha$, $B=\mathrm{diag}[\delta_i\mu_i^+ +(1-\delta_i)\mu_i^-]\in\mathbb{R}^{n\times n}$ with δ_i defined as

$$\delta_i=\begin{cases}1 & \text{if } \hat{\theta}_i^T\varphi(\hat{Z})\ge\beta_i\\ 0 & \text{Otherwise,}\end{cases} \tag{46}$$

and $\beta_i=\hat{\theta}_i^T\bar{\gamma}\varphi+\ell_i$ with ℓ_i defined in (33), $i=1,\ldots,n$.

Remark 3: A difference from switching function δ_i in (33) is that velocity signal x_2 in this section is estimated by a high-gain observer. Thus the switching function δ_i in (33) should be redesigned. According to (8), we can obtain $\hat{\theta}_i^T\varphi(Z)=\hat{\theta}_i^T\varphi(\hat{Z})-\hat{\theta}_i^T\bar{\gamma}\varphi$. Consider (8) and (33), we know that if $\delta_i=1$, it follows that $\hat{\theta}_i^T\varphi(Z)=\hat{\theta}_i^T\varphi(\hat{Z})-\hat{\theta}_i^T\bar{\gamma}\varphi\ge\ell_i$ and $\hat{\theta}_i^T\varphi(\hat{Z})\ge\hat{\theta}_i^T\bar{\gamma}\varphi+\ell_i$, and if $\delta_i=0$, it follows that $\hat{\theta}_i^T\varphi(Z)=\hat{\theta}_i^T\varphi(\hat{Z})-\hat{\theta}_i^T\bar{\gamma}\varphi<\ell_i$ and $\hat{\theta}_i^T\varphi(\hat{Z})<\hat{\theta}_i^T\bar{\gamma}\varphi+\ell_i$. Defining $\beta_i=\hat{\theta}_i^T\bar{\gamma}\varphi+\ell_i$, we can obtain the switching function δ_i in (46), $i=1,\ldots,n$.

Similar to analysis in Remark 1, we can conclude that $\mu_i, i=1,\ldots,n$ given in (43) are bounded, i.e., $\mu_{ci}^-\le\mu_i\le\mu_{ci}^+, i=1,\ldots,n$, are guaranteed. A Lyapunov function candidate is chosen as

$$V_3=\sum_{i=1}^n\ln(\cosh(z_{1i}))+\frac{1}{2}z_2^T M z_2+\frac{1}{2}\sum_{i=1}^n\tilde{\theta}_i^T\Gamma_i^{-1}\tilde{\theta}_i \tag{47}$$

Substituting (43)-(45) into the time derivative of (47), we further have

$$\begin{aligned}\dot{V}_3 =& -\sum_{i=1}^{n} k_i \ln(\cosh(z_{1i})) - \sum_{i=1}^{n} \tilde{\theta}_i^T(\varphi(\hat{Z})\hat{z}_{2i} + \varsigma\hat{\theta}_i)\\ &- z_2^T K_1 \tanh(\hat{z}_2) + z_2^T(B\tanh(B^{-1}\hat{\psi})\\ &- B\tanh(B^{-1}\psi) - p(\mu)) \end{aligned} \tag{48}$$

Similar with calculation in III-B, $B\tanh(B^{-1}\hat{\psi}) - B\tanh(B^{-1}\psi)$ can be simplified as $B_i\tanh(B_i^{-1}\hat{\psi}_i) - B_i\tanh(B_i^{-1}\psi_i) = (1-\tanh^2(\eta_i))(\hat{\psi}_i - \psi_i)$, where $\eta_i \in (B_i^{-1}\hat{\psi}_i, B_i^{-1}\psi_i)$ or $\eta_i \in (B_i^{-1}\psi_i, B_i^{-1}\hat{\psi}_i)$. With combination of (8), (29) and (44), we have $\hat{\psi}_i - \psi_i = \tilde{\theta}_i^T\varphi(Z) + \tilde{\theta}_i^T\bar{\gamma}\varphi + \theta_i^T\bar{\gamma}\varphi + \epsilon_i(Z)$, $i = 1,\ldots,n$. According to Taylor expansion, we know

$$\tanh(\hat{z}_2) = \hat{z}_2 + o(\hat{z}_2), \quad \|\hat{z}_2\| < \frac{\pi}{2} \tag{49}$$

where $o(\hat{z}_2) = -\frac{1}{3}\hat{z}_2^3 + \frac{2}{15}\hat{z}_2^5 - \frac{17}{315}\hat{z}_2^7 + \cdots$, and in the interval $\|\hat{z}_2\| < \frac{\pi}{2}$, $o(\hat{z}_2)$ is bounded, i.e., $\|o(\hat{z}_2)\| \le \bar{o}_c$ with $\bar{o}_c$ being a positive constant. Thus, (48) becomes

$$\begin{aligned}\dot{V}_3 =& -\sum_{i=1}^{n} k_i \ln(\cosh(z_{1i})) - \sum_{i=1}^{n} \tilde{\theta}_i^T(\varphi(\hat{Z})\hat{z}_{2i} + \varsigma\hat{\theta}_i)\\ &- z_2^T K_1 \hat{z}_2 - z_2^T K_1 o(\hat{z}_2) + z_2^T(I - \mathrm{Tanh}^2(\eta))\\ &\times(\tilde{\theta}^T\varphi(Z) + \tilde{\theta}^T\bar{\gamma}\varphi + \theta^T\bar{\gamma}\varphi + \epsilon(Z)) - z_2^T p(\mu) \end{aligned} \tag{50}$$

Note that

$$\begin{aligned}\tilde{z}_2 =& \frac{\pi_2}{\rho} - x_2 = \hat{x}_2 - x_2\\ =& (\hat{x}_2 - \alpha) - (x_2 - \alpha) = \hat{z}_2 - z_2 \end{aligned} \tag{51}$$

Thus, we have $-\sum_{i=1}^{n}\tilde{\theta}_i^T\varphi(\hat{Z})\hat{z}_{2i} + z_2^T\tilde{\theta}^T\varphi(Z) = -\sum_{i=1}^{n}\tilde{\theta}_i^T(\varphi(\hat{Z})\hat{z}_{2i} - \varphi(Z)z_{2i})$. Since $\varphi(\hat{Z}) = \varphi(Z) + \bar{\gamma}\varphi$, we have

$$\begin{aligned}&-\sum_{i=1}^{n}\tilde{\theta}_i^T\varphi(\hat{Z})\hat{z}_{2i} + z_2^T\tilde{\theta}^T\varphi(Z)\\ &= -\sum_{i=1}^{n}\tilde{\theta}_i^T(\varphi(Z)\hat{z}_{2i} + \bar{\gamma}\varphi\hat{z}_{2i} - \varphi(Z)z_{2i})\\ &= -\sum_{i=1}^{n}\tilde{\theta}_i^T(\varphi(Z)\tilde{z}_{2i} + \bar{\gamma}\varphi z_{2i} + \bar{\gamma}\varphi\tilde{z}_{2i}) \end{aligned} \tag{52}$$

Thus, we have

$$\begin{aligned}\dot{V}_3 =& -\sum_{i=1}^{n} k_i \ln(\cosh(z_{1i})) - z_2^T K_1 z_2 - \sum_{i=1}^{n}\tilde{\theta}_i^T\varsigma\hat{\theta}_i\\ &- z_2^T K_1\tilde{z}_2 - z_2^T K_1 o(\hat{z}_2) - \sum_{i=1}^{n}\tilde{\theta}_i^T(\varphi(Z)\tilde{z}_{2i} + \bar{\gamma}\varphi z_{2i}\\ &+ \bar{\gamma}\varphi\tilde{z}_{2i}) + 2|z_2^T(\tilde{\theta}^T\bar{\gamma}\varphi + \theta^T\bar{\gamma}\varphi + \epsilon(Z))|\\ &+ |z_2^T\tilde{\theta}^T\varphi(Z)| - z_2^T p(\mu) \end{aligned} \tag{53}$$

In terms of Young's inequality, we have $-z_2^T p(\mu) \le \frac{1}{2}z_2^T z_2 + \frac{1}{2}\bar{p}^2$, $-\sum_{i=1}^{n}\tilde{\theta}_i^T\varsigma\hat{\theta}_i \le -\frac{\varsigma}{2}\sum_{i=1}^{n}\tilde{\theta}_i^T\tilde{\theta}_i + \frac{\varsigma}{2}\sum_{i=1}^{n}\theta_i^T\theta_i$, $-z_2^T K_1\tilde{z}_2 \le \frac{1}{2}z_2^T z_2 + \frac{1}{2}\lambda_{\max}(K_1^T K_1)\bar{z}^2$, $z_2^T K_1 o(\hat{z}_2) \le \frac{1}{2}z_2^T z_2 + \frac{1}{2}\lambda_{\max}(K_1^T K_1)\bar{o}_c^2$, $-\sum_{i=1}^{n}\tilde{\theta}_i^T\varphi(Z)\tilde{z}_{2i} \le \frac{\varrho_2^2}{2}\sum_{i=1}^{n}\tilde{\theta}_i^T\tilde{\theta}_i + \frac{1}{2\varrho_2^2}l^2\bar{z}^2$, $-\sum_{i=1}^{n}\tilde{\theta}_i^T\bar{\gamma}\varphi z_{2i} \le \frac{\varrho_3^2}{2}\sum_{i=1}^{n}\tilde{\theta}_i^T\tilde{\theta}_i + \frac{\bar{\gamma}^2\|\varphi\|^2}{2\varrho_3^2}z_2^T z_2$, $-\sum_{i=1}^{n}\tilde{\theta}_i^T\bar{\gamma}\varphi\tilde{z}_{2i} \le \frac{\varrho_4^2}{2}\sum_{i=1}^{n}\tilde{\theta}_i^T\tilde{\theta}_i + \frac{\bar{\gamma}^2\|\varphi\|^2}{2\varrho_4^2}\bar{z}^2$, $|z_2^T\tilde{\theta}^T\varphi(Z)| \le \frac{\varrho_5^2}{2}\sum_{i=1}^{n}\tilde{\theta}_i^T\tilde{\theta}_i + \frac{l^2}{2\varrho_5^2}z_2^T z_2$, $|z_2^T\tilde{\theta}^T\bar{\gamma}\varphi| \le \frac{\varrho_3^2}{2}\sum_{i=1}^{n}\tilde{\theta}_i^T\tilde{\theta}_i + \frac{\bar{\gamma}^2\|\varphi\|^2}{2\varrho_3^2}z_2^T z_2$, $|z_2^T\theta^T\bar{\gamma}\varphi| \le \frac{\varrho_3^2}{2}\sum_{i=1}^{n}\theta_i^T\theta_i + \frac{\bar{\gamma}^2\|\varphi\|^2}{2\varrho_3^2}z_2^T z_2$, and $|z_2^T\epsilon(Z)| \le \frac{1}{2}z_2^T z_2 + \frac{1}{2}\bar{\epsilon}^2$. Therefore, we have

$$\begin{aligned}\dot{V}_3 \le& -\sum_{i=1}^{n} k_i \ln(\cosh(z_{1i})) - z_2^T\Bigg(K_1 - \frac{1}{2}(5 + \bar{\gamma}^2\|\varphi\|^2\\ &\times\frac{5}{\varrho_3^2} + \frac{l^2}{\varrho_5^2})I\Bigg)z_2 - \frac{1}{2}(\varsigma - \varrho_2^2 - 3\varrho_3^2 - \varrho_4^2 - \varrho_5^2)\sum_{i=1}^{n}\tilde{\theta}_i^T\tilde{\theta}_i\\ &+ \frac{1}{2}(\varsigma + 2\varrho_3^2)\sum_{i=1}^{n}\theta_i^T\theta_i + \frac{1}{2}\Bigg(\frac{l^2}{\varrho_2^2} + \frac{\bar{\gamma}^2\|\varphi\|^2}{\varrho_4^2}\\ &+ \lambda_{\max}(K_1^T K_1)\Bigg)\bar{z}^2 + \frac{1}{2}\lambda_{\max}(K_1^T K_1)\bar{o}_c^2 + \bar{\epsilon}^2 + \frac{1}{2}\bar{p}^2\\ \le& -\kappa_3 V_3 + C_3 \end{aligned} \tag{54}$$

where

$$\begin{aligned}\kappa_3 =& \min\Bigg\{\min_{i=1,\ldots,n} k_i, \frac{\lambda_{\min}\Big(2K_1 - (5 + \frac{5\bar{\gamma}^2\|\varphi\|^2}{\varrho_3^2} + \frac{l^2}{\varrho_5^2})I\Big)}{\lambda_{\max}(M)}\\ &\min_{i=1,\ldots,n}\Bigg(\frac{(\varsigma - \varrho_2^2 - 3\varrho_3^2 - \varrho_4^2 - \varrho_5^2)}{\lambda_{\max}(\Gamma_i^{-1})}\Bigg)\Bigg\}\\ C_3 =& \frac{1}{2}(\varsigma + 2\varrho_3^2)\sum_{i=1}^{n}\theta_i^T\theta_i + \frac{1}{2}\lambda_{\max}(K_1^T K_1)\bar{o}_c^2 + \bar{\epsilon}^2\\ &+ \frac{1}{2}\Bigg(\frac{l^2}{\varrho_2^2} + \frac{\bar{\gamma}^2\|\varphi\|^2}{\varrho_4^2} + \lambda_{\max}(K_1^T K_1)\Bigg)\bar{z}^2 + \frac{1}{2}\bar{p}^2 \end{aligned} \tag{55}$$

To guarantee $\kappa_3 > 0$, controller parameters should be chosen to satisfy: $\min_{i=1,\ldots,n} k_i > 0$, $\lambda_{\min}\Big(2K_1 - (5 + \frac{5\bar{\gamma}^2\|\varphi\|^2}{\varrho_3^2} + \frac{l^2}{\varrho_5^2})I\Big) > 0$ and $\Big((\varsigma - \varrho_2^2 - 3\varrho_3^2 - \varrho_4^2 - \varrho_5^2)\Big) > 0$, where ϱ_2, ϱ_3, ϱ_4 and ϱ_5 are adjustable positive parameters. Then the following theorem is obtained.

Theorem 3: For robotic system (1), by designing adaptive neural network controller (43) with adaptive law (45) and state observer (42), the controller can ensure that all the error signals are UUB. Furthermore, z_1 eventually converges to the compact set defined as $\Omega_{z_1} := \Big\{z_1 \in \mathbb{R}^n \big| |z_{1i}| \le \sqrt{2e^{H_3}}, i = 1,\ldots,n\Big\}$, and z_2 eventually converges to the compact set defined as $\Omega_{z_2} := \Big\{z_2 \in \mathbb{R}^n \big| \|z_2\| \le \sqrt{\frac{2H_3}{\lambda_{\min(M)}}}\Big\}$, where $H_3 = V_3(0) + \frac{C_3}{\kappa_3}$.

Proof: The proof is similar to that of Theorem 1, so it will not be discussed in details.

IV. Simulation

In this section, we will verify the effectiveness of the proposed control by implementing the numerical simulation. A typical robot with three degrees of freedom is considered, and three degrees of freedom are three rotary degrees. The system matrixes of the robot given in (1) are given by

$$M = \begin{bmatrix} M_{11} & M_{12} & M_{13} \\ M_{21} & M_{22} & M_{23} \\ M_{31} & M_{32} & M_{33} \end{bmatrix} \tag{56}$$

$$C = \begin{bmatrix} C_{11} & C_{12} & C_{13} \\ C_{21} & C_{22} & C_{23} \\ C_{31} & C_{32} & C_{33} \end{bmatrix}, G = \begin{bmatrix} G_1 \\ G_2 \\ G_3 \end{bmatrix} \tag{57}$$

where $M_{11} = m_3 q_3^2 \sin^2(q_2) + p_1$; $D_{12} = p_2 q_3 \cos(q_2)$; $M_{13} = p_2 \sin(q_2)$; $M_{21} = p_2 q_3 \cos(q_2)$; $M_{22} = m_3 q_3^2 + I_2$; $M_{23} = 0$; $M_{31} = p_2 \sin(q_2)$; $M_{32} = 0$; $M_{33} = m_3$; $C_{11} = p_4 \dot{q}_2 + p_5 \dot{q}_3$; $C_{12} = p_4 \dot{q}_1 - p_3 q_3 p_8$; $C_{13} = p_5 \dot{q}_1 - p_3 p_6 q_3$; $C_{21} = -p_4 \dot{q}_1$; $C_{22} = m_3 q_3 \dot{q}_3$; $C_{23} = p_3 p_9 - m_3 q_3 \dot{q}_2$; $C_{31} = -p_5 \dot{q}_1 + p_3 p_{10}$; $C_{32} = m_3 q_3 \dot{q}_2 + p_3 p_{11}$; $C_{33} = 0$; $G_1 = 0$; $G_2 = -m_3 g q_3 \cos(q_2)$; $G_3 = -m_3 g \sin(q_2)$. where $p_1 = m_3 l_2^2 + m_2 l_1^2 + I_1$; $p_2 = m_3 l_2$; $p_3 = m_3 l_1$; $p_4 = m_3 q_3^2 \sin(q_2) \cos(q_2)$; $p_5 = m_3 q_3^2 \sin^2(q_2)$; $p_6 = \sin(q_2)\dot{q}_2$;$p_7 = \sin(q_2)\dot{q}_3$; $p_8 = p_6 + p_7$; $p_9 = \cos(q_2)\dot{q}_1$; $p_{10} = \cos(q_2)\dot{q}_2$ and $p_{11} = \cos(q_2)\dot{q}_3$. Parameters of the robotic system are defined in the table below.

Table 1: Parameters of the robot

Parameter	Description	Value
m_1	Mass of link 1	2.00 kg
m_2	Mass of link 2	1.00 kg
m_3	Mass of link 3	0.30 kg
l_1	Length of link 1	1.00 m
l_2	Length of link 2	0.20 m
l_3	Length of link 3	1.00 m
I_1	Inertia of link 1	0.5×10^{-3} kgm^2
I_2	Inertia of link 2	0.1×10^{-3} kgm^2

The detailed simulation results are given as follows.

A. Model-based Control Simulation Implementation

In this section, the effectiveness of model-based control (23) will be verified by simulation implementation. Initial values are set as: $x_1(0) = [0.05, 0.56, -0.05]^T$rad and $x_2(0) = [0, 0, 0]^T$rad/s. Controller parameters are chosen as follows: $K = \text{diag}[100, 100, 100]$, $K_1 = \text{diag}[10, 10, 10]$, $\mu_1^+ = 1$, $\mu_2^+ = 2$, $\mu_3^+ = 2$, $\mu_1^- = -2$, $\mu_2^- = -1$ and $\mu_3^- = -2$. Therefore observing (23), we know

$$-13Nm \le \mu_1 \le 12Nm \tag{58}$$

$$-12Nm \le \mu_2 \le 13Nm \tag{59}$$

$$-13Nm \le \mu_3 \le 13Nm \tag{60}$$

The reference trajectory of x_1 is set as $x_d = [0.5\sin(t), 0.6\cos(t), 0.7\sin(t)]^T$rad.

The detailed simulation results are given in Figs. 1-3. In Fig. 1, actual trajectory x_1 and reference trajectory x_d are plotted, respectively, and Fig. 1 also illustrates that x_1 fast converges to a small neighborhood of reference trajectory x_d, which shows that the tracking performance of the robot is satisfactory. In Fig. 2, tracking error z_1 is plotted, and it can be known that z_1 converges to a small neighborhood of zero with a satisfactory overshoot. In Fig. 3, control input μ is given and is constrained in the predefined region, i.e., $\mu_{ci}^- \le \mu_i \le \mu_{ci}^+$, $i = 1, 2, 3$, are satisfied.

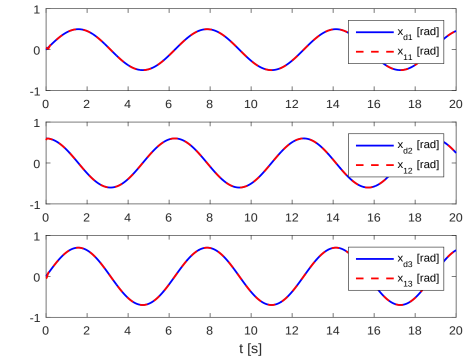

Fig. 1. Actual trajectory x_1 and reference trajectory x_d under model-based control (23).

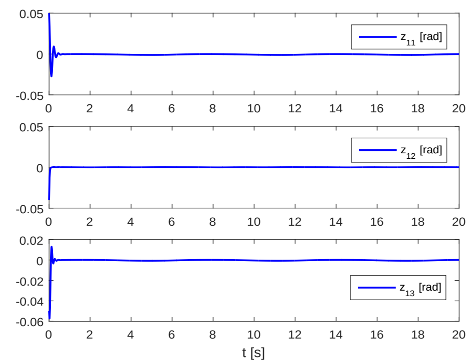

Fig. 2. Tracking error $z_1 = x_1 - x_d$ under model-based control (23).

B. State-Feedback-Based Adaptive Neural Control Simulation Implementation

In this section, the effectiveness of proposed control (30) will be verified by simulation implementation. The number of neural nodes is set as $l = 2^{12}$, the center of activation function $\psi(Z)$ is chosen in the area of $[-1,1]\times[-1,1]\times[-1,1]\times[-1,1]\times[-1,1]\times[-1,1]\times[-1,1]\times[-1,1]\times[-1,1]\times[-1,1]\times[-1,1]\times[-1,1]$. The width of centers is set as $\eta^2 = 1$. Initial values are set as $\hat{\theta}_1(0) = \hat{\theta}_2(0) = \hat{\theta}_3(0) = [0, \ldots, 0]^T \in \mathbb{R}^{2^{12}}$. The parameters of the updating law given in (32) are set as $\Gamma_1 = \text{diag}[100, 100, 100]$, $\Gamma_2 = \text{diag}[50, 50, 50]$, $\Gamma_3 = \text{diag}[100, 100, 100]$ and $\varsigma = 0.0001$. The rest of controller parameters are the same as those of section IV-A.

The detailed simulation results are given in Figs. 4-7. In Fig. 4, actual trajectory x_1 and reference trajectory x_d are plotted, respectively, and Fig. 4 shows that x_1 converges to a small neighborhood of reference trajectory x_d, which shows that the tracking performance of the robot is satisfactory. In Fig. 5, tracking error z_1 is given. Fig. 6 plots control input μ and furthermore μ is constrained in the the predefined region, i.e., $\mu_{ci}^- \le \mu_i \le \mu_{ci}^+$, $i = 1, 2, 3$, are satisfied. Fig. 7 gives the Euclidean norm of weight vector $\hat{\theta}_i$, $i = 1, 2, 3$. By observing the above-mentioned analysis, we know that although there exist unknown dynamics $M(q)$, $C(q, \dot{q})$ and $G(q)$, adaptive neural control (30) constrained within the predefined region, still makes the robot have a satisfactory tracking performance, which has been illustrated by simulation results.

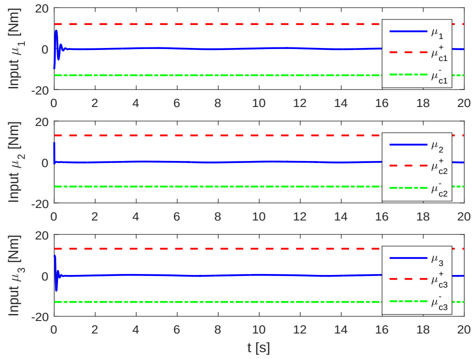

Fig. 3. Control input μ under model-based control (23).

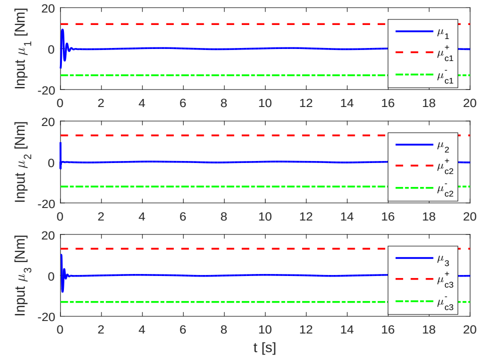

Fig. 6. Control input μ under state-feedback-based adaptive neural control (30).

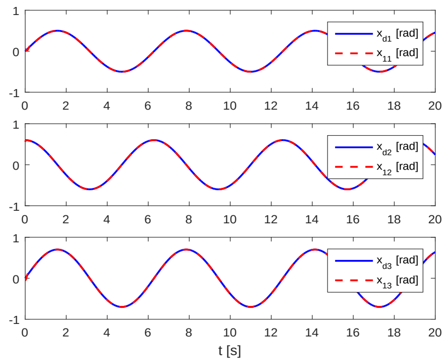

Fig. 4. Actual trajectory x_1 and reference trajectory x_d under state-feedback-based adaptive neural control (30).

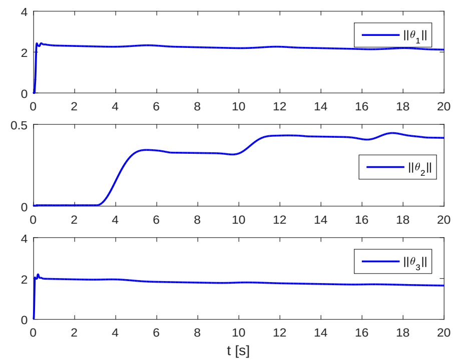

Fig. 7. Euclidean norm $\|\hat{\theta}_i\|, i = 1, 2, 3$ under state-feedback-based adaptive neural control (30).

C. Output-Feedback-Based Adaptive Neural Control Simulation Implementation

In this section, the effectiveness of proposed control (43) will be verified by simulation implementation. High-gain observer parameters are set as $\lambda_1 = 1$ and $\rho = 0.0007$. The rest of controller parameters are the same as those of section IV-B.

The detailed simulation results are given in Figs. 8-11. In Fig. 8, actual trajectory x_1 and reference trajectory x_d are plotted, respectively, and Fig. 8 also illustrates that x_1 converges to a small neighborhood of reference trajectory x_d, which shows that the tracking performance of the robot is satisfactory. In Fig. 9, tracking error z_1 is given. Fig. 10 plots control input μ which is constrained in the the predefined region, i.e., $\mu_{ci}^- \leq \mu_i \leq \mu_{ci}^+$, $i = 1, 2, 3$, have been guaranteed. Fig. 11 gives the Euclidean norm of weight vector $\hat{\theta}_i$, $i = 1, 2, 3$. By observing the above-mentioned analysis, we know that although there exist unknown dynamics $M(q)$, $C(q, \dot{q})$, $G(q)$ and immeasurable state x_2, proposed control (43) constrained within the predefined region, still makes the robot have a satisfactory tracking performance, which has been

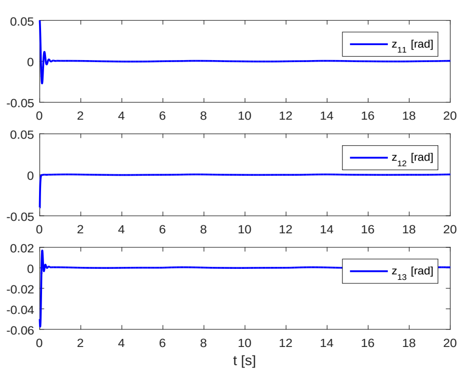

Fig. 5. Tracking error $z_1 = x_1 - x_d$ under state-feedback-based adaptive neural control (30).

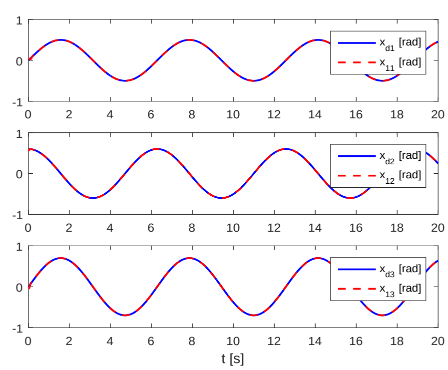

Fig. 8. Actual trajectory x_1 and reference trajectory x_d under output-feedback-based adaptive neural control (43).

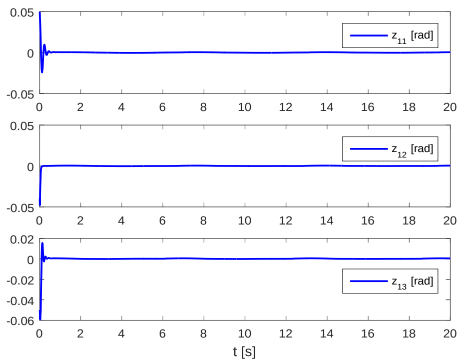

Fig. 9. Tracking error $z_1 = x_1 - x_d$ under output-feedback-based adaptive neural control (43).

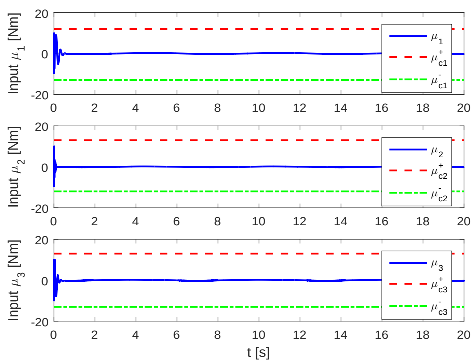

Fig. 10. Control input μ under output-feedback-based adaptive neural control (43).

illustrated by simulation results.

V. Conclusion

In this paper, an adaptive neural network bounded control scheme is developed for an n-link rigid robotic manipulator with unknown dynamics. For methods of dealing with saturation in [66]–[70], the bounds of the designed controller cannot be known *a prior* for the designer. In this paper, the bounds of the designed controller are known *a prior* and furthermore they can be changed by adjusting control gains, *making them applicable within actuator limitations*. Furthermore, it should be emphasized that the bounds of the designed controller are asymmetric. Neural networks are used to approximate unknown robotic dynamics. The effectiveness of the proposed scheme has been verified by simulation results. It should be emphasized that robots in practice are often required to move in a finite space, which illustrates that output constraint [75] should be guaranteed. Therefore, the optimal algorithm, such as parallel algorithm [76], [77], I-Ching divination evolutionary algorithm [78], [79] and dynamic programming [80]–[82], will be investigated for robots with output constraint in the future.

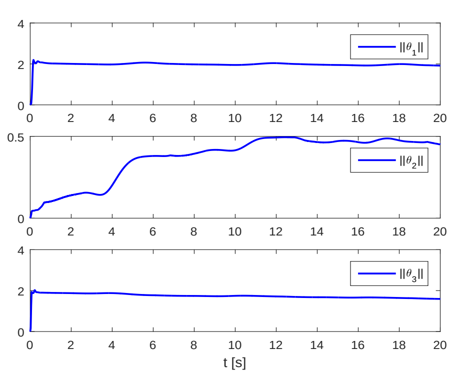

Fig. 11. Euclidean norm $\|\hat{\theta}_i\|, i = 1, 2, 3$ under output-feedback-based adaptive neural control (43).

Acknowledgement

The authors would like to thank the Editor-In-Chief, the Associate Editor and the anonymous reviewers for their constructive comments which helped improve the quality and presentation of this paper.

Appendix

Proof: Multiplying (28) by $e^{\kappa_1 t}$ equals $\frac{d(V_1 e^{\kappa_1 t})}{dt} \leq C_1 e^{\kappa_1 t}$. Integrating the above inequality, we get

$$V_1 \leq (V_1(0) - \frac{C_1}{\kappa_1})e^{-\kappa_1 t} + \frac{C_1}{\kappa_1} \leq V_1(0) + \frac{C_1}{\kappa_1} \tag{A.1}$$

Combining (21), we have

$$\ln(\cosh(z_{1i})) \leq \sum_{i=1}^{n} \ln(\cosh(z_{1i})) \leq V_1(0) + \frac{C_1}{\kappa_1} \tag{A.2}$$

$$\frac{1}{2}\lambda_{\min}(M)||z_2||^2 \leq \frac{1}{2} z_2^T M z_2 \leq V_1(0) + \frac{C_1}{\kappa_1} \tag{A.3}$$

Note that

$$\frac{1}{2} z_{1i}^2 \leq \cosh(z_{1i}) \tag{A.4}$$

we have

$$|z_{1i}| \leq \sqrt{2e^{H_1}},\ i = 1, \ldots, n \tag{A.5}$$

$$||z_2||^2 \leq \frac{2H_1}{\lambda_{\min}(M)} \tag{A.6}$$

where $H_1 = V_1(0) + \frac{C_1}{\kappa_1}$. This finishes the proof.

References

[1] W. He, Z. Li, and C. L. P. Chen, "A survey of human-centered intelligent robots:issues and challenges," *IEEE/CAA Journal of Automatica Sinica*, vol. 4, no. 4, pp. 602–609, 2017.

[2] R. Cui, L. Chen, C. Yang, and M. Chen, "Extended state observer-based integral sliding mode control for an underwater robot with unknown disturbances and uncertain nonlinearities," *IEEE Transactions on Industrial Electronics*, vol. 64, pp. 6785–6795, Aug 2017.

[3] A. Sciutti, M. Mara, V. Tagliasco, and G. Sandini, "Humanizing human-robot interaction: On the importance of mutual understanding," *IEEE Technology and Society Magazine*, vol. 37, pp. 22–29, March 2018.

[4] P. Huang, F. Zhang, J. Cai, D. Wang, Z. Meng, and J. Guo, "Dexterous tethered space robot: Design, measurement, control, and experiment," *IEEE Transactions on Aerospace and Electronic Systems*, vol. 53, pp. 1452–1468, June 2017.

[5] H. Wang, C. Wang, W. Chen, X. Liang, and Y. Liu, "Three-dimensional dynamics for cable-driven soft manipulator," *IEEE/ASME Transactions on Mechatronics*, vol. 22, pp. 18–28, Feb 2017.

[6] M. Chen, "Disturbance attenuation tracking control for wheeled mobile robots with skidding and slipping," *IEEE Transactions on Industrial Electronics*, vol. 64, pp. 3359–3368, April 2017.

[7] H. Chen, L. Chen, Q. Zhang, and F. Tong, "Visual servoing of dynamic wheeled mobile robots with anti-interference finite-time controllers," *Assembly Automation*, vol. 38, no. 5, pp. 558–567, 2018.

[8] L. Pan, G. Bao, F. Xu, and L. Zhang, "Adaptive robust sliding mode trajectory tracking control for 6 degree-of-freedom industrial assembly robot with disturbances," *Assembly Automation*, vol. 38, no. 3, pp. 259–267, 2018.

[9] W. He, W. Ge, Y. Li, Y. J. Liu, C. Yang, and C. Sun, "Model identification and control design for a humanoid robot," *IEEE Transactions on Systems Man & Cybernetics Systems*, vol. 47, no. 1, pp. 45–57, 2017.

[10] Z. Li, C. Su, G. Li, and H. Su, "Fuzzy approximation-based adaptive backstepping control of an exoskeleton for human upper limbs," *IEEE Transactions on Fuzzy Systems*, vol. 23, no. 3, pp. 555–566, 2015.

[11] C. Yang, X. Wang, L. Cheng, and H. Ma, "Neural-learning-based telerobot control with guaranteed performance," *IEEE Transactions on Cybernetics*, vol. 47, no. 10, pp. 3148–3159, 2017.

[12] Z. Li, B. Huang, A. Ajoudani, C. Yang, C. Su, and A. Bicchi, "Asymmetric bimanual control of dual-arm exoskeletons for human-cooperative manipulations," *IEEE Transactions on Robotics*, vol. 34, pp. 264–271, Feb 2018.

[13] Z. Li, T. Zhao, F. Chen, Y. Hu, C. Su, and T. Fukuda, "Reinforcement learning of manipulation and grasping using dynamical movement primitives for a humanoidlike mobile manipulator," *IEEE/ASME Transactions on Mechatronics*, vol. 23, pp. 121–131, Feb 2018.

[14] K. D. Kallu, W. Jie, and M. C. Lee, "Sensorless reaction force estimation of the end effector of a dual-arm robot manipulator using sliding mode control with a sliding perturbation observer," *International Journal of Control, Automation and Systems*, vol. 16, pp. 1367–1378, Jun 2018.

[15] S. Dai, S. He, H. Lin, and C. Wang, "Platoon formation control with prescribed performance guarantees for usvs," *IEEE Transactions on Industrial Electronics*, vol. 65, pp. 4237–4246, May 2018.

[16] Y. H. Kim and F. L. Lewis, "Neural network output feedback control of robot manipulators," *IEEE Transactions on Robotics & Automation*, vol. 15, no. 2, pp. 301–309, 1999.

[17] C. Yang, K. Huang, H. Cheng, Y. Li, and C. Y. Su, "Haptic identification by elm-controlled uncertain manipulator," *IEEE Transactions on Systems Man & Cybernetics Systems*, vol. 47, no. 8, pp. 2398–2409, 2017.

[18] H. Qiao, M. Wang, J. Su, S. Jia, and R. Li, "The concept of attractive region in environment and its application in high-precision tasks with low-precision systems," *IEEE/ASME Transactions on Mechatronics*, vol. 20, pp. 2311–2327, Oct 2015.

[19] S. L. Dai, M. Wang, and C. Wang, "Neural learning control of marine surface vessels with guaranteed transient tracking performance," *IEEE Transactions on Industrial Electronics*, vol. 63, no. 3, pp. 1717–1727, 2016.

[20] Z. Zhang, S. Xu, and B. Zhang, "Exact tracking control of nonlinear systems with time delays and dead-zone input," *Automatica*, vol. 52, pp. 272 – 276, 2015.

[21] Z. Zhang, S. Xu, and B. Zhang, "Asymptotic tracking control of uncertain nonlinear systems with unknown actuator nonlinearity," *IEEE Transactions on Automatic Control*, vol. 59, pp. 1336–1341, May 2014.

[22] B. Xu and Y. Shou, "Composite learning control of mimo systems with applications," *IEEE Transactions on Industrial Electronics*, vol. 65, pp. 6414–6424, Aug 2018.

[23] B. Xu, "Composite learning finite-time control with application to quadrotors," *IEEE Transactions on Systems, Man, and Cybernetics: Systems*, vol. 48, pp. 1806–1815, Oct 2018.

[24] Z. Peng, J. Wang, and J. Wang, "Constrained control of autonomous underwater vehicles based on command optimization and disturbance estimation," *IEEE Transactions on Industrial Electronics*, pp. 1–1, 2018.

[25] Z. Peng, J. Wang, and D. Wang, "Containment maneuvering of marine surface vehicles with multiple parameterized paths via spatial-temporal decoupling," *IEEE/ASME Transactions on Mechatronics*, vol. 22, pp. 1026–1036, April 2017.

[26] Y. Song and X. Yuan, "Low-cost adaptive fault-tolerant approach for semiactive suspension control of high-speed trains," *IEEE Transactions on Industrial Electronics*, vol. 63, pp. 7084–7093, Nov 2016.

[27] Y. Song, X. Huang, and C. Wen, "Tracking control for a class of unknown nonsquare mimo nonaffine systems: A deep-rooted information based robust adaptive approach," *IEEE Transactions on Automatic Control*, vol. 61, no. 10, pp. 3227–3233, 2016.

[28] R. Cui, C. Yang, Y. Li, and S. Sharma, "Adaptive neural network control of auvs with control input nonlinearities using reinforcement learning," *IEEE Transactions on Systems, Man, and Cybernetics: Systems*, vol. 47, pp. 1019–1029, June 2017.

[29] C. L. P. Chen and Z. Liu, "Broad learning system: An effective and efficient incremental learning system without the need for deep architecture," *IEEE Transactions on Neural Networks and Learning Systems*, vol. 29, pp. 10–24, Jan 2018.

[30] N. Wang, M. J. Er, J. C. Sun, and Y. C. Liu, "Adaptive robust online constructive fuzzy control of a complex surface vehicle system," *IEEE Transactions on Cybernetics*, vol. 46, pp. 1511–1523, July 2016.

[31] C. L. P. Chen, C. E. Ren, and T. Du, "Fuzzy observed-based adaptive consensus tracking control for second-order multiagent systems with heterogeneous nonlinear dynamics," *IEEE Transactions on Fuzzy Systems*, vol. 24, no. 4, pp. 906–915, 2016.

[32] C. L. P. Chen, G. X. Wen, Y. J. Liu, and Z. Liu, "Observer-based adaptive backstepping consensus tracking control for high-order nonlinear semi-strict-feedback multiagent systems," *IEEE Transactions on Cybernetics*, vol. 46, pp. 1591–1601, July 2016.

[33] Z. Peng, D. Wang, and J. Wang, "Predictor-based neural dynamic surface control for uncertain nonlinear systems in strict-feedback form," *IEEE Transactions on Neural Networks and Learning Systems*, vol. 28, pp. 2156–2167, Sept 2017.

[34] S. Jung, "Improvement of tracking control of a sliding mode controller for robot manipulators by a neural network," *International Journal of Control, Automation and Systems*, vol. 16, pp. 937–943, Apr 2018.

[35] Y. Zhang, J. Sun, H. Liang, and H. Li, "Event-triggered adaptive tracking control for multiagent systems with unknown disturbances," *IEEE Transactions on Cybernetics*, pp. 1–12, 2018.

[36] H. Qiao, J. Peng, Z. . Xu, and B. Zhang, "A reference model approach to stability analysis of neural networks," *IEEE Transactions on Systems, Man, and Cybernetics, Part B (Cybernetics)*, vol. 33, pp. 925–936, Dec 2003.

[37] B. Xu, D. Yang, Z. Shi, Y. Pan, B. Chen, and F. Sun, "Online recorded data-based composite neural control of strict-feedback systems with application to hypersonic flight dynamics," *IEEE Transactions on Neural Networks and Learning Systems*, vol. 29, pp. 3839–3849, Aug 2018.

[38] Y. J. Liu, J. Li, S. Tong, and C. L. P. Chen, "Neural network control-based adaptive learning design for nonlinear systems with full-state constraints," *IEEE Transactions on Neural Networks and Learning Systems*, vol. 27, pp. 1562–1571, July 2016.

[39] H. Yang and J. Liu, "An adaptive rbf neural network control method for a class of nonlinear systems," *IEEE/CAA Journal of Automatica Sinica*, vol. 5, no. 2, pp. 457–462, 2018.

[40] H. Li, L. Bai, L. Wang, Q. Zhou, and H. Wang, "Adaptive neural control of uncertain nonstrict-feedback stochastic nonlinear systems with output constraint and unknown dead zone," *IEEE Transactions on Systems Man & Cybernetics Systems*, vol. 47, no. 8, pp. 2048–2059, 2017.

[41] P. Huang, D. Wang, Z. Meng, F. Zhang, and Z. Liu, "Impact dynamic modeling and adaptive target capturing control for tethered space robots with uncertainties," *IEEE/ASME Transactions on Mechatronics*, vol. 21, pp. 2260–2271, Oct 2016.

[42] Z. Zhao, J. Shi, X. Lan, X. Wang, and J. Yang, "Adaptive neural network control of a flexible string system with non-symmetric dead-zone and output constraint," *Neurocomputing*, vol. 283, pp. 1 – 8, 2018.

[43] Z. Peng, D. Wang, H. Zhang, and G. Sun, "Distributed neural network control for adaptive synchronization of uncertain dynamical multiagent systems," *IEEE Transactions on Neural Networks and Learning Systems*, vol. 25, pp. 1508–1519, Aug 2014.

[44] C. Mu, Z. Ni, C. Sun, and H. He, "Air-breathing hypersonic vehicle tracking control based on adaptive dynamic programming," *IEEE Transactions on Neural Networks and Learning Systems*, vol. 28, pp. 584–598, March 2017.

[45] L. Cheng, W. Liu, Z. Hou, J. Yu, and M. Tan, "Neural-network-based nonlinear model predictive control for piezoelectric actuators," *IEEE Transactions on Industrial Electronics*, vol. 62, pp. 7717–7727, Dec 2015.

[46] F. Zouari, A. Ibeas, A. Boulkroune, J. Cao, and M. M. Arefi, "Adaptive neural output-feedback control for nonstrict-feedback time-delay fractional-order systems with output constraints and actuator nonlinearities," *Neural Networks*, vol. 105, pp. 256 – 276, 2018.

[47] F. Zouari, A. Boulkroune, and A. Ibeas, "Neural adaptive quantized output-feedback control-based synchronization of uncertain time-delay incommensurate fractional-order chaotic systems with input nonlinearities," *Neurocomputing*, vol. 237, pp. 200 – 225, 2017.

[48] M. Chen and G. Tao, "Adaptive fault-tolerant control of uncertain nonlinear large-scale systems with unknown dead zone," *IEEE Transactions on Cybernetics*, vol. 46, no. 8, pp. 1851–1862, 2016.

[49] B. Gao and W. Han, "Neural network model reference decoupling control for single leg joint of hydraulic quadruped robot," *Assembly Automation*, vol. 38, no. 4, pp. 465–475, 2018.

[50] Y. Cheng, Y. Wang, H. Yu, Y. Zhang, J. Zhang, Q. Yang, H. Sheng, and L. Bai, "Solenoid model for visualizing magnetic flux leakage testing of complex defects," *NDT & E International*, vol. 100, pp. 166 – 174, 2018.

[51] D. P. Li, Y. J. Liu, S. Tong, C. L. P. Chen, and D. J. Li, "Neural networks-based adaptive control for nonlinear state constrained systems with input delay," *IEEE Transactions on Cybernetics*, pp. 1–10, 2018.

[52] Y. J. Liu, S. Tong, C. L. P. Chen, and D. J. Li, "Adaptive nn control using integral barrier lyapunov functionals for uncertain nonlinear block-triangular constraint systems," *IEEE Transactions on Cybernetics*, vol. 47, pp. 3747–3757, Nov 2017.

[53] Y. J. Liu and S. Tong, "Barrier lyapunov functions-based adaptive control for a class of nonlinear pure-feedback systems with full state constraints ," *Automatica*, vol. 64, no. 2, pp. 70–75, 2016.

[54] S. Zhang, Y. Dong, Y. Ouyang, Z. Yin, and K. Peng, "Adaptive neural control for robotic manipulators with output constraints and uncertainties," *IEEE Transactions on Neural Networks and Learning Systems*, vol. 29, pp. 5554–5564, Nov 2018.

[55] J. Peng, F. Xin, and C. Ying, "Response of a swirlmeter to oscillatory flow," *Flow Measurement & Instrumentation*, vol. 19, no. 2, pp. 107–115, 2008.

[56] J. Peng, X. Fu, and Y. Chen, "Experimental investigations of strouhal number for flows past dual triangulate bluff bodies," *Flow Measurement & Instrumentation*, vol. 19, no. 6, pp. 350–357, 2008.

[57] Q. Zhou, P. Shi, H. Liu, and S. Xu, "Neural-network-based decentralized adaptive output-feedback control for large-scale stochastic nonlinear systems," *IEEE Transactions on Systems, Man, and Cybernetics, Part B (Cybernetics)*, vol. 42, pp. 1608–1619, Dec 2012.

[58] W. He, S. S. Ge, Y. Li, E. Chew, and Y. S. Ng, "Neural network control of a rehabilitation robot by state and output feedback," *Journal of Intelligent & Robotic Systems*, vol. 80, no. 1, pp. 15–31, 2015.

[59] T.-C. Lee, K.-T. Song, C.-H. Lee, and C.-C. Teng, "Tracking control of unicycle-modeled mobile robots using a saturation feedback controller," *IEEE Transactions on Control Systems Technology*, vol. 9, pp. 305–318, March 2001.

[60] Q. Zhou, H. Li, L. Wang, and R. Lu, "Prescribed performance observer-based adaptive fuzzy control for nonstrict-feedback stochastic nonlinear systems," *IEEE Transactions on Systems, Man, and Cybernetics: Systems*, vol. 48, pp. 1747–1758, Oct 2018.

[61] L. Wang, M. V. Basin, H. Li, and R. Lu, "Observer-based composite adaptive fuzzy control for nonstrict-feedback systems with actuator failures," *IEEE Transactions on Fuzzy Systems*, vol. 26, pp. 2336–2347, Aug 2018.

[62] Q. Zhou, C. Wu, and P. Shi, "Observer-based adaptive fuzzy tracking control of nonlinear systems with time delay and input saturation," *Fuzzy Sets and Systems*, vol. 316, pp. 49 – 68, 2017.

[63] Z. Zhao, Y. Liu, and F. Luo, "Output feedback boundary control of an axially moving system with input saturation constraint," *ISA Transactions*, vol. 68, pp. 22 – 32, 2017.

[64] B. Zhu, C. Meng, and G. Hu, "Robust consensus tracking of double-integrator dynamics by bounded distributed control," *International Journal of Robust & Nonlinear Control*, vol. 26, no. 7, pp. 1489–1511, 2016.

[65] T. Meng and W. He, "Iterative learning control of a robotic arm experiment platform with input constraint," *IEEE Transactions on Industrial Electronics*, vol. 65, no. 1, pp. 664–672, 2017.

[66] H. Min, S. Xu, Q. Ma, B. Zhang, and Z. Zhang, "Composite-observer-based output-feedback control for nonlinear time-delay systems with input saturation and its application," *IEEE Transactions on Industrial Electronics*, vol. 65, pp. 5856–5863, July 2018.

[67] W. Wang and S. Tong, "Adaptive fuzzy bounded control for consensus of multiple strict-feedback nonlinear systems.," *IEEE Transactions on Cybernetics*, vol. 48, no. 2, pp. 522–531, 2018.

[68] J. Ma, S. S. Ge, Z. Zheng, and D. Hu, "Adaptive nn control of a class of nonlinear systems with asymmetric saturation actuators," *IEEE Transactions on Neural Networks & Learning Systems*, vol. 26, no. 7, pp. 1532–1538, 2015.

[69] Q. Zhou, L. Wang, C. Wu, H. Li, and H. Du, "Adaptive fuzzy control for nonstrict-feedback systems with input saturation and output constraint," *IEEE Transactions on Systems Man & Cybernetics Systems*, vol. 47, no. 1, pp. 1–12, 2017.

[70] H. Li, J. Wang, and P. Shi, "Output-feedback based sliding mode control for fuzzy systems with actuator saturation," *IEEE Transactions on Fuzzy Systems*, vol. 24, pp. 1282–1293, Dec 2016.

[71] C. Yang, T. Teng, B. Xu, Z. Li, J. Na, and C. Y. Su, "Global adaptive tracking control of robot manipulators using neural networks with finite-time learning convergence," *International Journal of Control Automation & Systems*, no. 11, pp. 1–9, 2017.

[72] S. S. Ge, T. H. Lee, and C. J. Harris, *Adaptive Neural Network Control of Robotic Manipulators*. WORLD SCIENTIFIC, 1998.

[73] S. S. Ge, C. C. Hang, H. L. Tong, and T. Zhang, "Stable adaptive neural network control," *Springer International*, vol. 13, 2001.

[74] W. He, X. He, and C. Sun, "Vibration control of an industrial moving strip in the presence of input deadzone," *IEEE Transactions on Industrial Electronics*, vol. 64, pp. 4680–4689, June 2017.

[75] W. He, S. S. Ge, and D. Huang, "Modeling and vibration control for a nonlinear moving string with output constraint," *IEEE/ASME Transactions on Mechatronics*, vol. 20, pp. 1886–1897, Aug 2015.

[76] F. Wang, J. Zhang, Q. Wei, X. Zheng, and L. Li, "Pdp: parallel dynamic programming," *IEEE/CAA Journal of Automatica Sinica*, vol. 4, pp. 1–5, Jan 2017.

[77] F. Wang, N. Zheng, D. Cao, C. M. Martinez, L. Li, and T. Liu, "Parallel driving in cpss: a unified approach for transport automation and vehicle intelligence," *IEEE/CAA Journal of Automatica Sinica*, vol. 4, no. 4, pp. 577–587, 2017.

[78] C. L. P. Chen, T. Zhang, L. Chen, and S. C. Tam, "I-ching divination evolutionary algorithm and its convergence analysis," *IEEE Transactions on Cybernetics*, vol. 47, pp. 2–13, Jan 2017.

[79] T. Zhang, C. L. P. Chen, L. Chen, X. Xu, and B. Hu, "Design of highly nonlinear substitution boxes based on i-ching operators," *IEEE Transactions on Cybernetics*, vol. 48, pp. 3349–3358, Dec 2018.

[80] G. Wu, J. Sun, and J. Chen, "Optimal linear quadratic regulator of switched systems," *IEEE Transactions on Automatic Control*, pp. 1–1, 2018.

[81] B. Gao, P. Lu, W. L. Woo, G. Y. Tian, Y. Zhu, and M. Johnston, "Variational bayesian sub-group adaptive sparse component extraction for diagnostic imaging system," *IEEE Transactions on Industrial Electronics*, vol. 65, no. 10, pp. 8142–8152, 2018.

[82] B. Gao, X. Li, W. L. Woo, and G. y. Tian, "Physics-based image segmentation using first order statistical properties and genetic algorithm for inductive thermography imaging," *IEEE Transactions on Image Processing*, vol. 27, pp. 2160–2175, May 2018.

Linghuan Kong received the B.Eng. degree in automation from the College of Engineering, Qufu Normal University, Rizhao, China, in 2016 and the M.Eng. degree in control engineering from the School of Automation Engineering, University of Electronic Science and Technology of China, Chengdu, China, in 2019. He is currently pursuing the Ph.D. degree in control science and engineering with the School of Automation and Electrical Engineering, University of Science and Technology Beijing, Beijing, China.

His current research interests include robotics, neural network control, and adaptive control.

Wei He (S'09-M'12-SM'16) received his B.Eng. in automation and his M.Eng. degrees in control science and engineering from from College of Automation Science and Engineering, South China University of Technology (SCUT), China, in 2006 and 2008, respectively, and his Ph.D. degree in control science and engineering from from Department of Electrical & Computer Engineering, the National University of Singapore (NUS), Singapore, in 2011.

He is currently working as a full professor in School of Automation and Electrical Engineering, University of Science and Technology Beijing, Beijing, China. He has co-authored 2 books published in Springer and published over 100 international journal and conference papers. He was awarded a Newton Advanced Fellowship from the Royal Society, UK in 2017. He was a recipient of the IEEE SMC Society Andrew P. Sage Best Transactions Paper Award in 2017. He is serving the Chair of IEEE SMC Society Beijing Capital Region Chapter. He is serving as an Associate Editor of *IEEE Transactions on Neural Networks and Learning Systems*, *IEEE Transactions on Control Systems Technology*, *IEEE Transactions on Systems, Man, and Cybernetics: Systems*, *IEEE/CAA Journal of Automatica Sinica*, *Neurocomputing*, and an Editor of *Journal of Intelligent & Robotic Systems*.

His current research interests include robotics, distributed parameter systems and intelligent control systems.

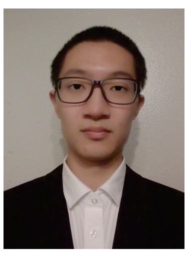

Yiting Dong (S'14) received the B.Eng. degree from the School of Automation Engineering, University of Electronic Science and Technology of China (UESTC), Chengdu, China, in 2014 and the M.Eng. degree in control science and engineering from UESTC, in 2017. He is currently pursuing the Ph.D. degree in mechanical engineering in the Department of Mechanical Engineering, Texas Tech University, Lubbock, TX, USA.

His current research interests include robust control, robotic control, and power electronics control.

Long Cheng (SM'14) received the B.S. (Hons.) degree in control engineering from Nankai University, Tianjin, China, in 2004, and the Ph.D. (Hons.) degree in control theory and control engineering from the Institute of Automation, Chinese Academy of Sciences, Beijing, China, in 2009.

He is currently a Full Professor with the Institute of Automation, Chinese Academy of Sciences. He is also an adjunct Professor with University of Chinese Academy of Sciences. He has published over 100 technical papers in peer-refereed journals and prestigious conference proceedings. He was a recipient of the IEEE Transactions on Neural Networks Outstanding Paper Award from IEEE Computational Intelligence Society, the Aharon Katzir Young Investigator Award from International Neural Networks Society and the Young Researcher Award from Asian Pacific Neural Networks Society. He is currently serving as an Associate Editor/Editorial Board Member of *IEEE Transactions on Cybernetics*, *Neural Processing Letters*, *Neurocomputing*, *International Journal of Systems Science*, and *Acta Automatica Sinica*.

His current research interests include the rehabilitation robot, intelligent control and neural networks.

Chenguang Yang (M'10-SM'16) is a Professor of Robotics. He received the B.Eng. degree in measurement and control from Northwestern Polytechnical University, Xi'an, China, in 2005, and the Ph.D. degree in control engineering from the National University of Singapore, Singapore, in 2010. He received postdoctoral training at Imperial College London, UK, from 2009 to 2010. He was awarded Marie Curie International Incoming Fellowship, EPSRC Innovation Fellowship, and the Best Paper Award of the IEEE Transactions on Robotics as well as over ten conference Best Paper Awards.

His research interest lies in human robot interaction and intelligent system design.

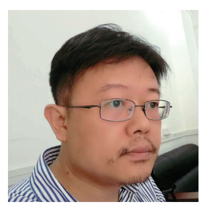

Zhijun Li (M'07-SM'09) received the Ph.D. degree in mechatronics, Shanghai Jiao Tong University, P. R. China, in 2002. From 2003 to 2005, he was a postdoctoral fellow in Department of Mechanical Engineering and Intelligent systems, The University of Electro-Communications, Tokyo, Japan. From 2005 to 2006, he was a research fellow in the Department of Electrical and Computer Engineering, National University of Singapore, and Nanyang Technological University, Singapore. Since 2012, he was a Professor in College of Automation Science and Engineering, South China University of Technology, Guangzhou, China. From 2017, he is a Professor in Department of Automation, University of Science and Technology, Hefei, China.

From 2016, he has been the Co-Chairs of IEEE SMC Technical Committee on Bio-mechatronics and Bio-robotics Systems (B^2S), and IEEE-RAS Technical Committee on Neuro-Robotics Systems. He is serving as an Editor-at-large of Journal of Intelligent & Robotic Systems, and Associate Editors of several IEEE Transactions.

Dr. Li's current research interests include wearable robotics, tele-operation systems, nonlinear control, neural network optimization, etc.